Star Cluster searches

Detecting new star clusters in the contemporary era

Methods to detect star clusters

- Usually utilized in conjunction
- Visual $\rightarrow$ searching for stellar overdensities or 'seeds'
- Star-counting (dividing the sky into bins and searching for enhancements in star count)
- Radial number density profiles (RDPs) and radial velocities
- Color-magnitude diagrams comparisons
- Parallaxes (distances), proper motions, radial velocities

'Seeds'

- Massive stars or massive star formation indications (YSOs, masers, etc.) → **all** or **almost all** massive stars form in star clusters (beware of the wording!)

- Various type of nebulae (HII regions, mid-infrared nebulae, supernova remnants?)

- Catalog 'seeds' → cataloged compact extended sources from older and/or lower resolution surveys (2MASS, WISE), possible misclassified galaxies in the Galactic plane
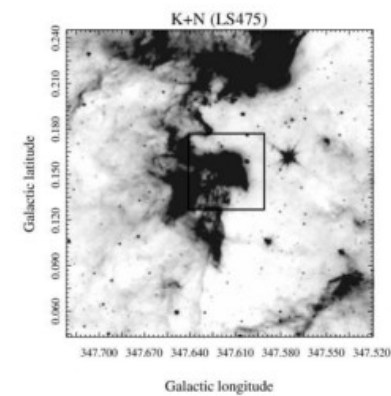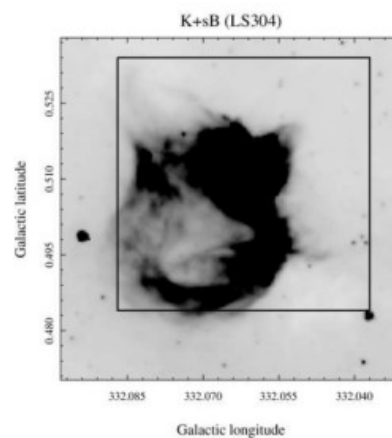
M 103 (credit: APOD)

??

Cas A

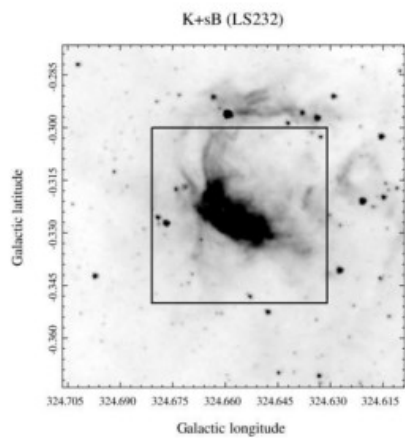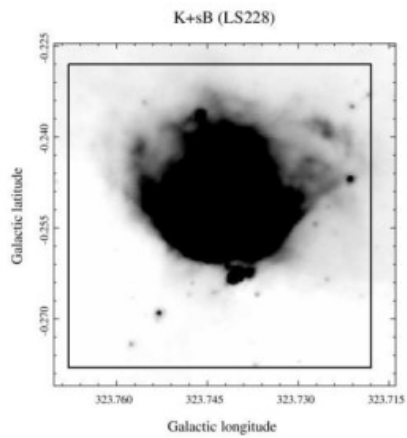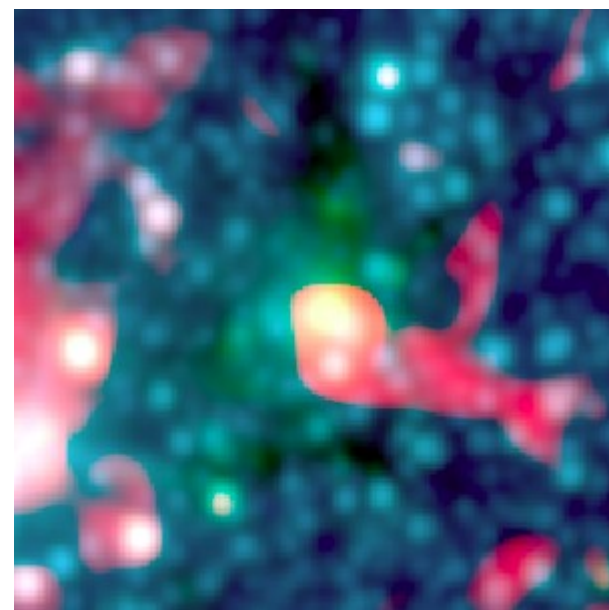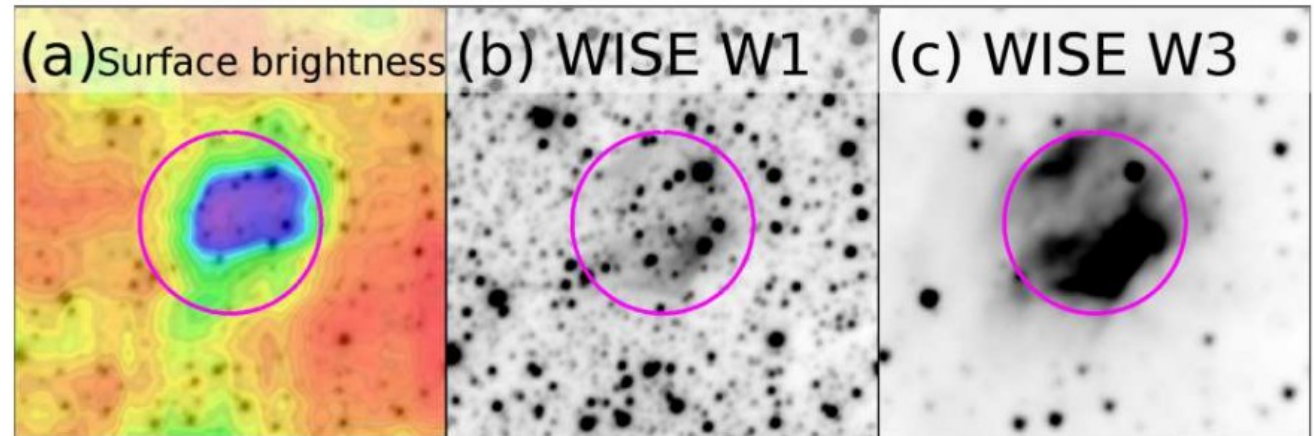K+sB (LS228)   K+sB (LS232)   K+sB (LS304)   K+N (LS475)
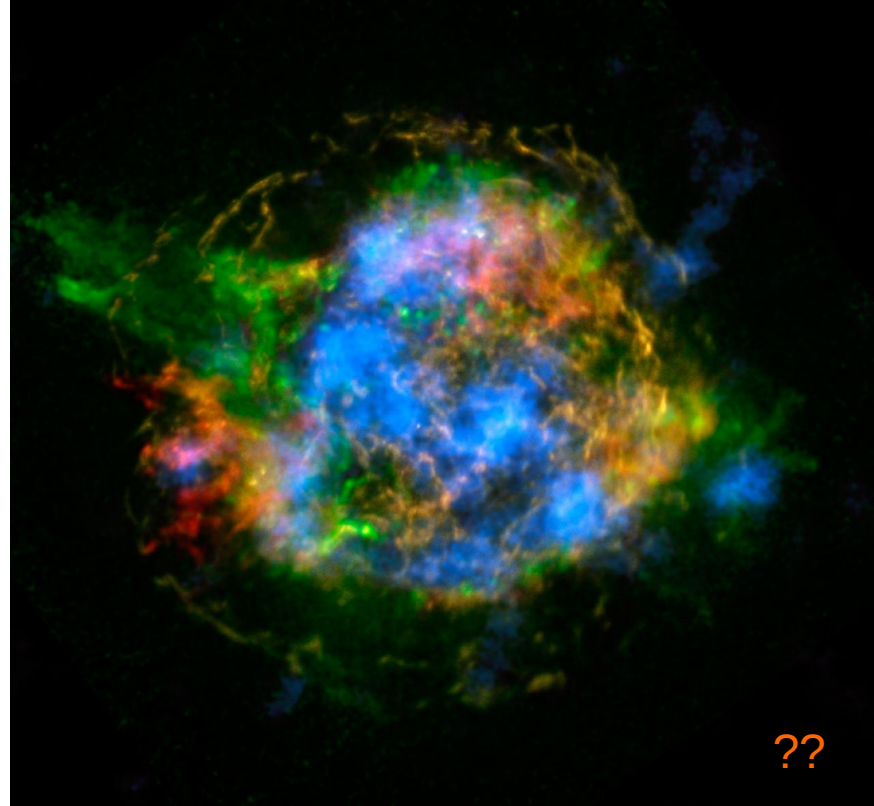
Fig. 9: Examples of different cluster morphologies based on images in the $8\,\mu$m band obtained with the Infrared Array Camera (IRAC) on board the Spizer Space Telescope. Boxes inside each panel correspond to the cluster candidate charts showed in Figure 1.

Barba+ (2015)
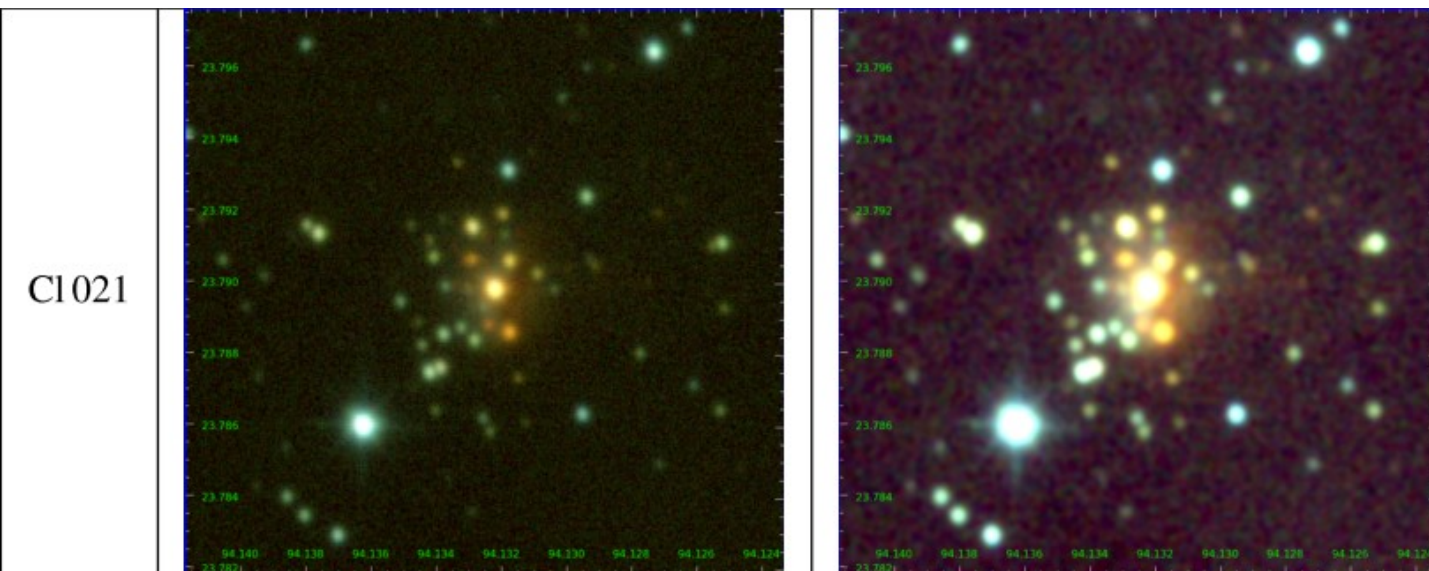
Survey exploitation

ra207.9981 (preliminary)

Ryu 010

Figure 3. (a) Smoothed surface brightness map of W1 image, (b) W1 image, and (c) W3 image of a new cluster sample, R. 010. The field of view of each image is $10' \times 10'$. Circles represent the apparent size of this cluster ($R = 2'.3$). North is up, a east is left.

Ryu & Lee (2018)

Cl 021

Compact cluster with red nebulous star dominating emission; coinciding with IRAS source;

Froebrich (2017)

OCs toward the inner Galaxy

References	Used dataset	Total $N_{cluster}$
Harris (1996, globular clusters)	Compiled[a]	157
Dias et al. (2002, open clusters)	Compiled[a]	2174
Nagata et al. (1990)	IRTF(NIR)[b]	1
Nagata et al. (1995)	IRTF(NIR)[b]	1
Bica et al. (2003a)	Compiled[a]	276
Bica et al. (2003b)	2MASS(NIR)	167
Dutra et al. (2003)	2MASS(NIR)	179
Mercer et al. (2005)	GLIMPSE(MIR)	92
Froebrich et al. (2007)	2MASS(NIR)	1021
Gutermuth et al. (2008)	$Spitzer$(MIR)[c]	1
Alexander et al. (2009)	GLIMPSE(MIR)	1
Negueruela et al. (2010)	UKIDSS(NIR)	1
Borissova et al. (2011)	VVV(NIR)	96
Moni Bidin et al. (2011)	VVV(NIR)	3
Negueruela et al. (2011)	2MASS(NIR)	1
González-Fernández & Negueruela (2012)	2MASS(NIR)	1
Solin et al. (2012)	UKIDSS(NIR)	137
Froebrich (2013)	NIR surveys[d]	6
Majaess (2013)	WISE(MIR)	229
Morales et al. (2013)	GLIMPSE(MIR)	75
Borissova et al. (2014)	VVV(NIR)	58
Solin et al. (2014)	VVV(NIR)	88
Barba et al. (2015)	VVV(NIR)	493
Camargo et al. (2016)	WISE(MIR)	1098[e]

Credit: Ryu & Lee (2018)

Methods to detect star clusters

- Usually utilized in conjunction

- Visual → searching for stellar overdensities or 'seeds'

- Star-counting (dividing the sky into bins and searching for enhancements in star count)

- Radial number density profiles (RDPs) and radial velocities

- Color-magnitude diagrams comparisons

- Parallaxes (distances), proper motions, radial velocities

Gaia 1 (star-counting)
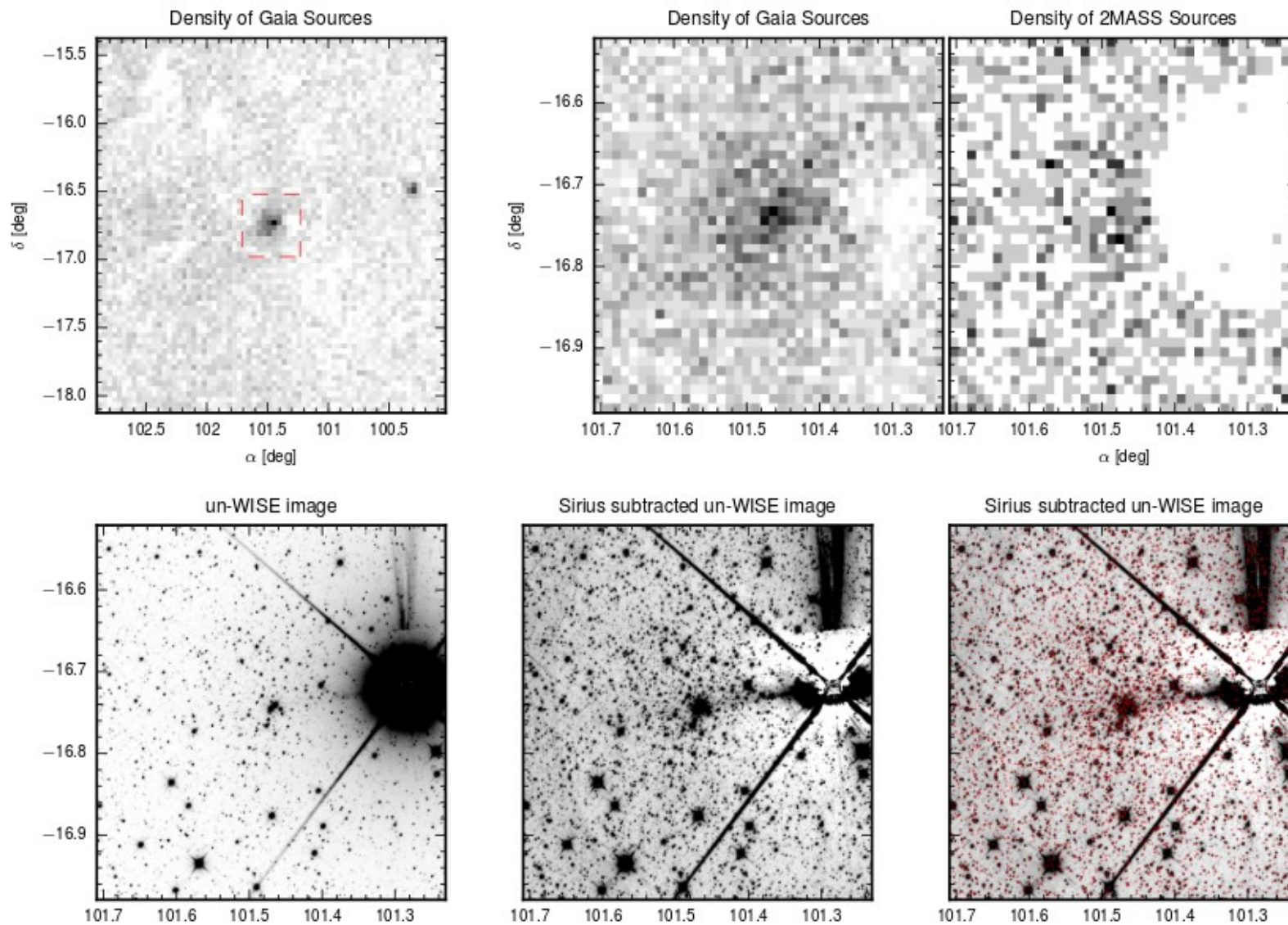
Figure 3. Distribution of sources around Gaia 1. *Top left:* The density of all *Gaia* sources with $G < 20$ within ~ 3 degrees of Gaia 1. The overdensity on the right edge of the panel is Berkeley 25, an old open cluster. The red box indicates the size of the region shown on other panels of the figure. *Top middle:* The density of *Gaia* sources with $G < 20$ in the $\sim 30' \times 30'$ field of view around Gaia 1. *Top right:* The density of the 2MASS sources in the same field of view. *Bottom left:* The $30' \times 30'$ image from the WISE survey showing Gaia 1. *Bottom middle:* The same image with the PSF of Sirius subtracted. *Bottom right:* The same image with *Gaia* source positions overplotted in red.
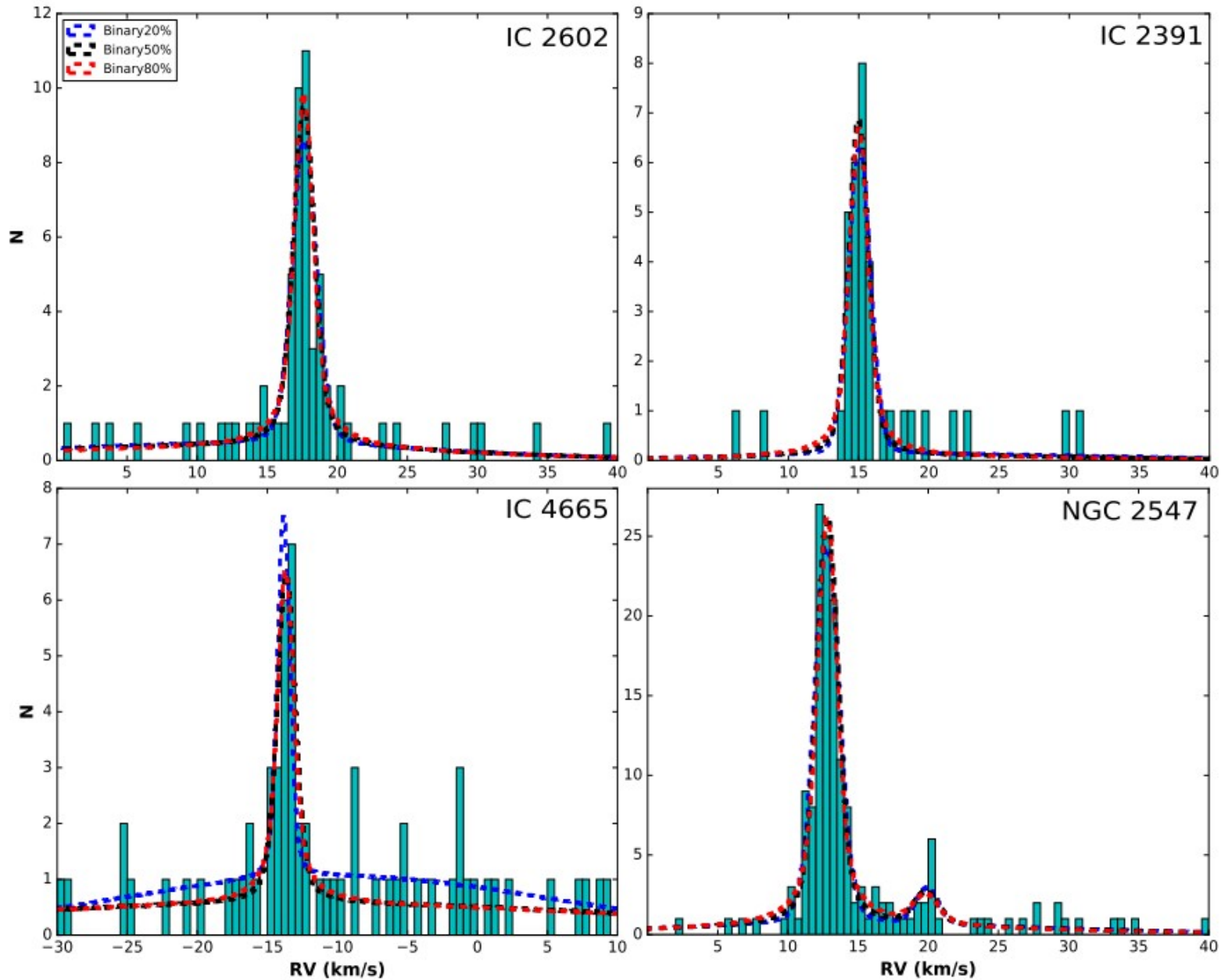
Koposov+ (2017)

Methods to detect star clusters

- Usually utilized in conjunction
- Visual → searching for stellar overdensities or 'seeds'
- Star-counting (dividing the sky into bins and searching for enhancements in star count)
- Radial number density profiles (RDPs) and radial velocities
- Color-magnitude diagrams comparisons
- Parallaxes (distances), proper motions, radial velocities

Radial density profiles

Piatti (2017)
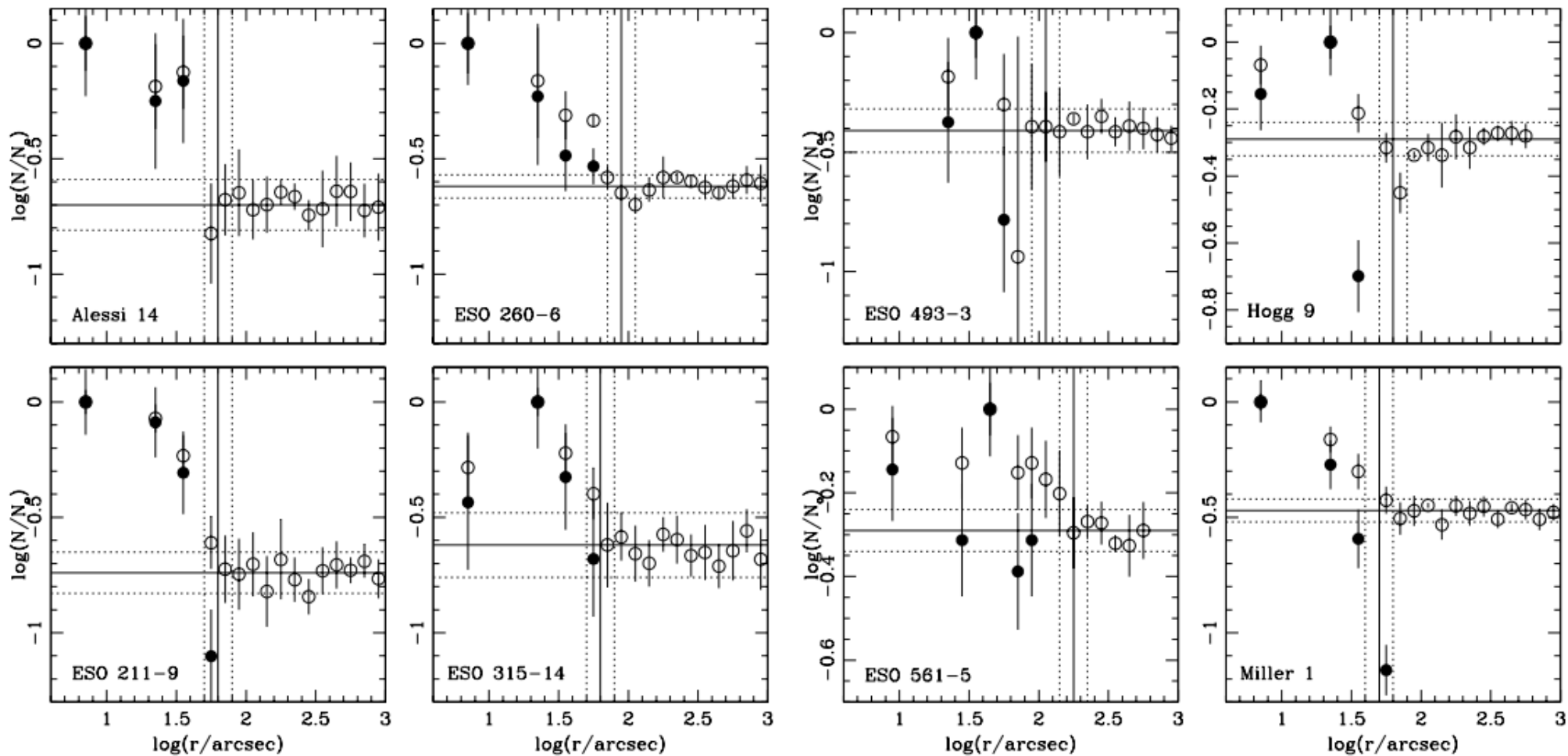
Radial velocities

Fig. 4. Radial velocity distribution. The blue, black and red dashed lines represent the fits performed by setting the binary fraction to 0.2, 0.5, and 0.8y, respectively.

Bravi+ (2018)

Methods to detect star clusters

- Usually utilized in conjunction

- Visual $\rightarrow$ searching for stellar overdensities or 'seeds'

- Star-counting (dividing the sky into bins and searching for enhancements in star count)

- Radial number density profiles (RDPs) and radial velocities

- Color-magnitude diagrams comparisons

- Parallaxes (distances), proper motions, radial velocities

Color-magnitude diagram analysis
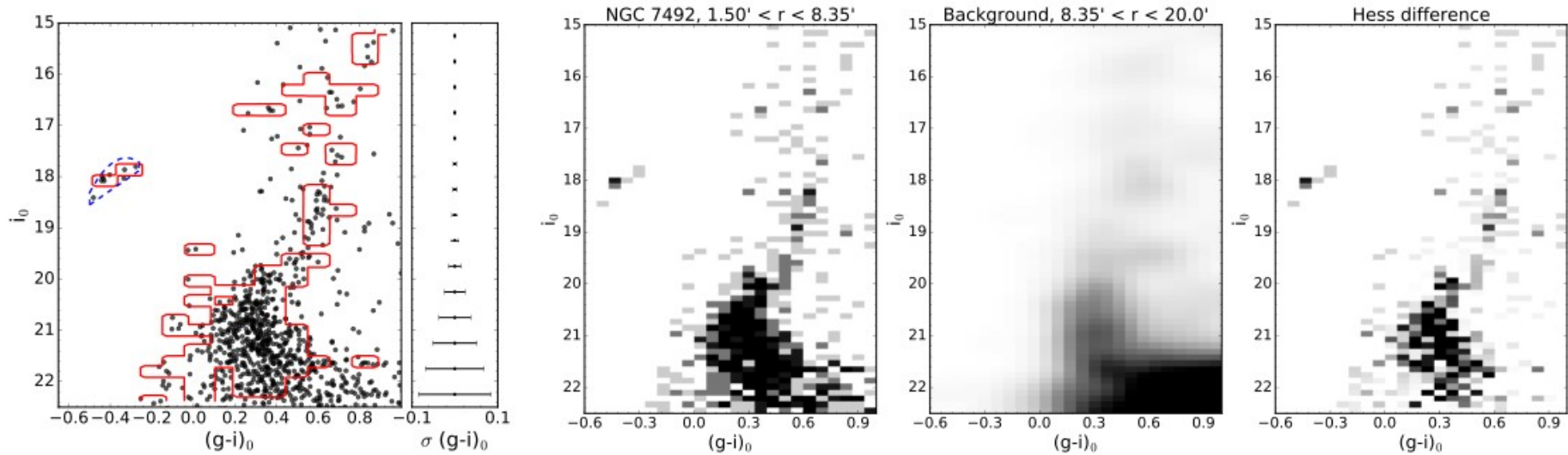
Figure 1. *First panel:* Extinction-corrected $(g - i, i)$ color-magnitude diagram of NGC 7492. It only includes stars within the tidal radius of the cluster ($r_t = 8.35'$), excluding the innermost center. The blue polygon encloses the BHB population of the cluster. The red contours show the color-magnitude bins where the matched filter selected stars in a $4 \times 4°$ field around the cluster fall into. The right inset shows the mean $(g - i)$ color photometric error as a function of i magnitude. Note that the apparent scatter around the cluster's CMD is larger than the photometric errors. Some of the contamination must come from the Galactic foreground/background (shown in the third panel). *Second panel:* Hess diagram for stars inside the tidal radius of the cluster, but excluding the innermost $1.5'$. *Third panel:* Hess diagram for stars with $8.35' < r < 20.0'$ away from the cluster's center. Sgr stream could provide some contribution to the MS and MSTO region of this CMD. *Fourth panel:* Hess difference. A number of familiar stellar populations can be identified in the second and fourth panels: MS, TO and HB as well as sparsely populated blue straggler sequence. In the background subtracted Hess diagram most of the contamination is removed and the sequences are much narrower.

Navarrete+ (2017)
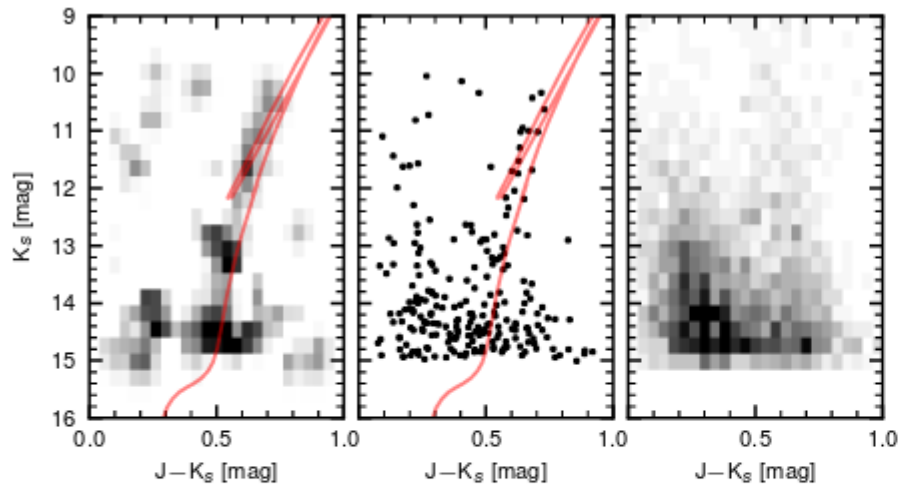
Gaia 2

Figure 7. *Left panel:* The background subtracted and extinction corrected 2MASS Hess diagram of Gaia 2 within central 3′. The PARSEC isochrone with the age of 8 Gyr and [Fe/H]= −0.6 at a distance modulus of 14.65 is overlaid in red. *Middle panel:* The 2MASS colour-magnitude diagram of Gaia 2 within 3′ of centre. Right panel: The Hess diagram of the background stars in the 12′, 24′ annulus.
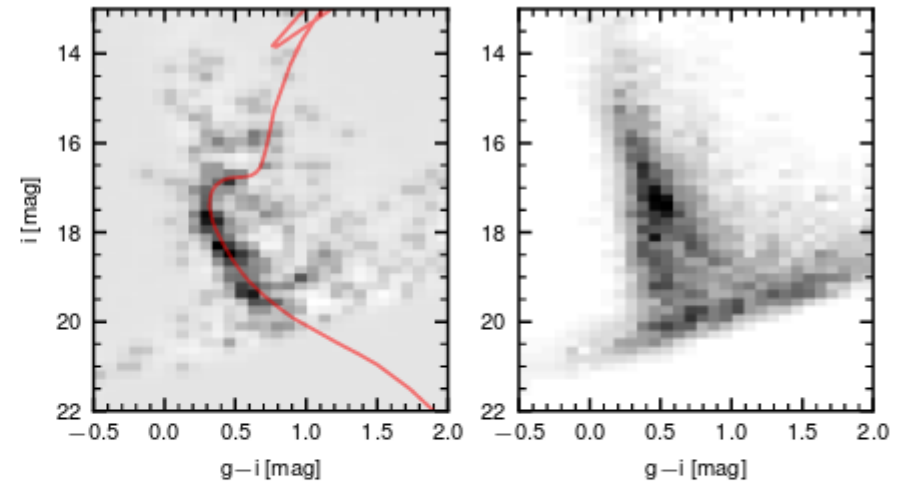
Figure 8. *Left panel:* The background subtracted and extinction corrected PS1 Hess diagram of Gaia 2 within central 3′. The PARSEC isochrone with the age of 8 Gyr and [Fe/H]= −0.6 at a distance modulus of 14.65 is overlaid in red. Right panel: The Hess diagram of the background stars in the 12′, 24′ annulus.

Koposov+ (2017)

Methods to detect star clusters

- Usually utilized in conjunction
- Visual → searching for stellar overdensities or 'seeds'
- Star-counting (dividing the sky into bins and searching for enhancements in star count)
- Radial number density profiles (RDPs) and radial velocities
- Color-magnitude diagrams comparisons
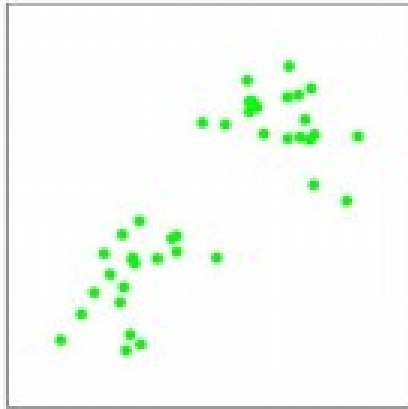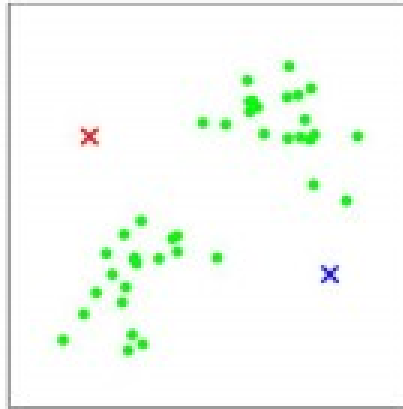- Parallaxes (distances), proper motions, radial velocities

Clustering
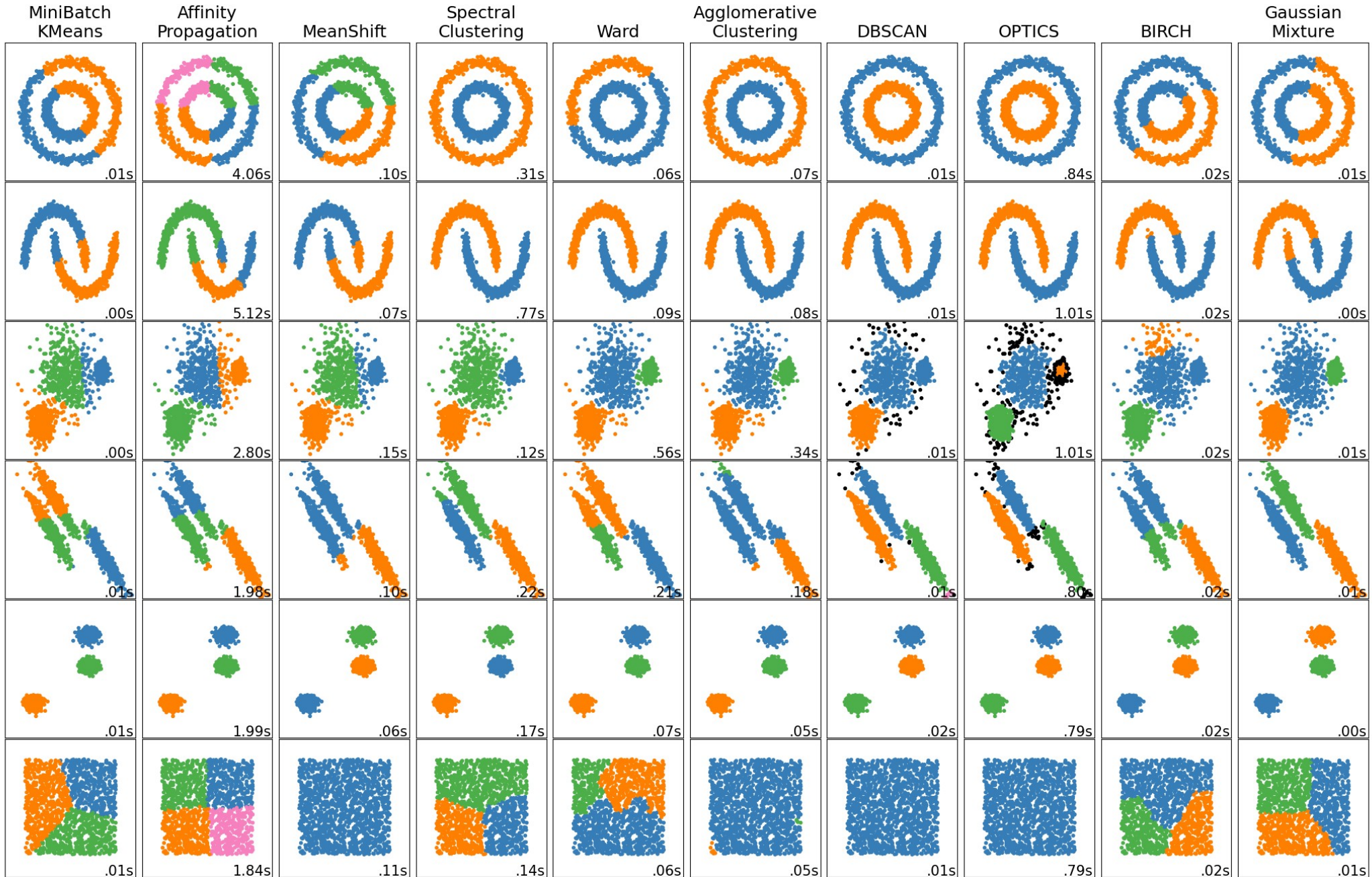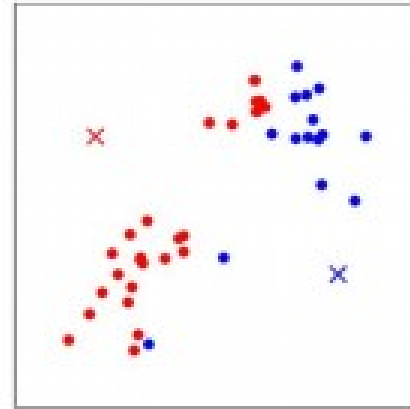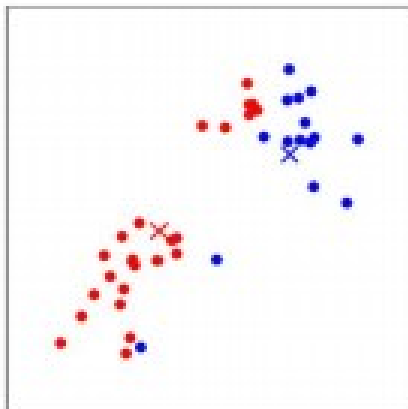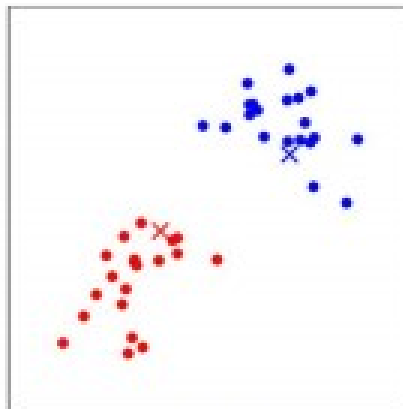

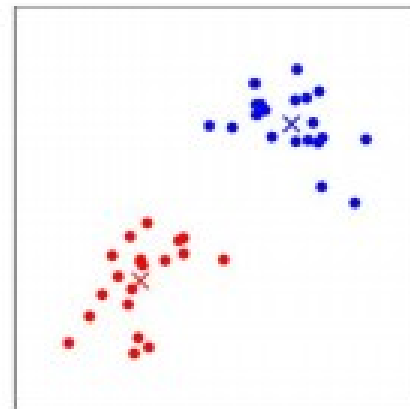Which one is the most appropriate algorithm?

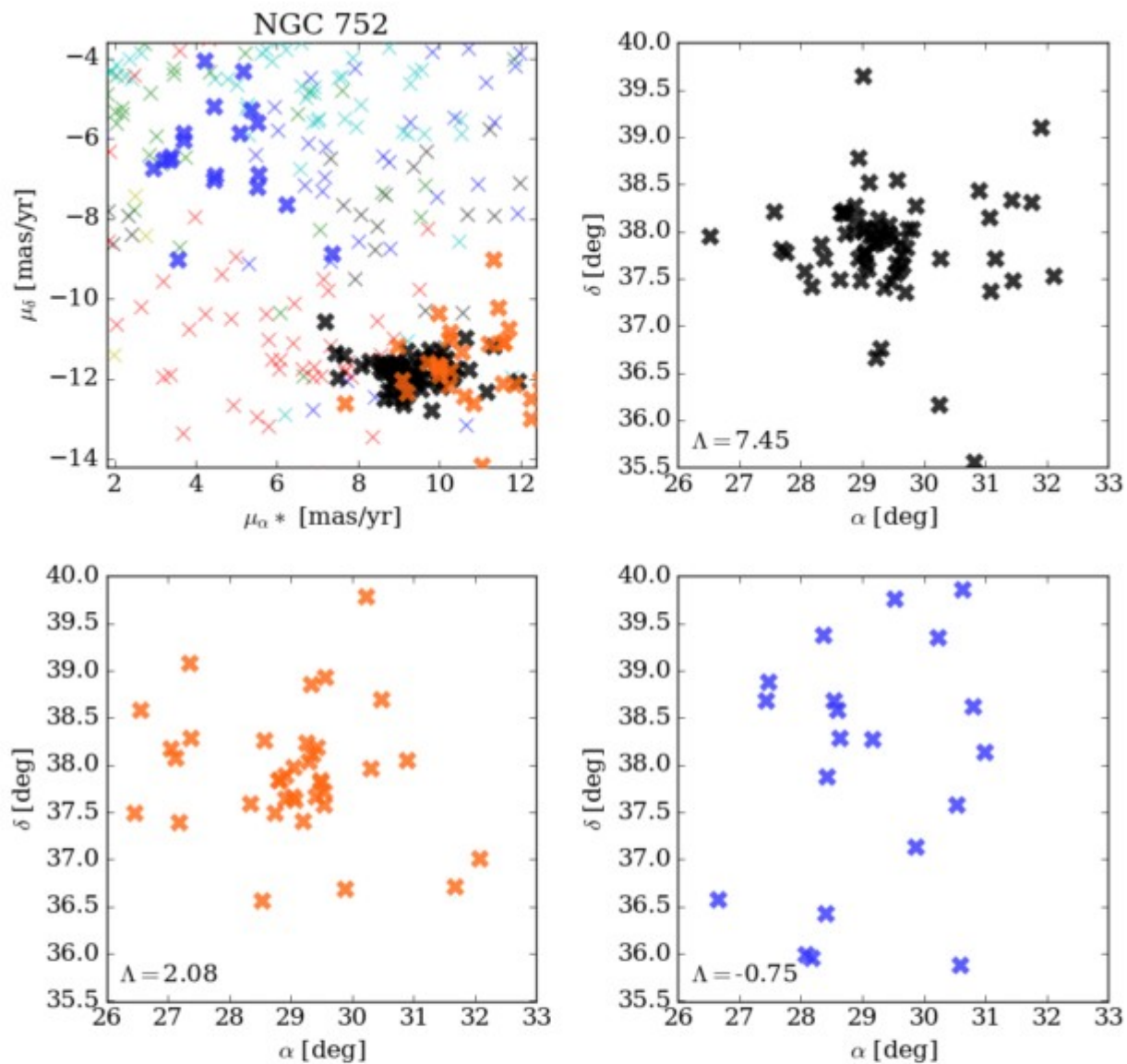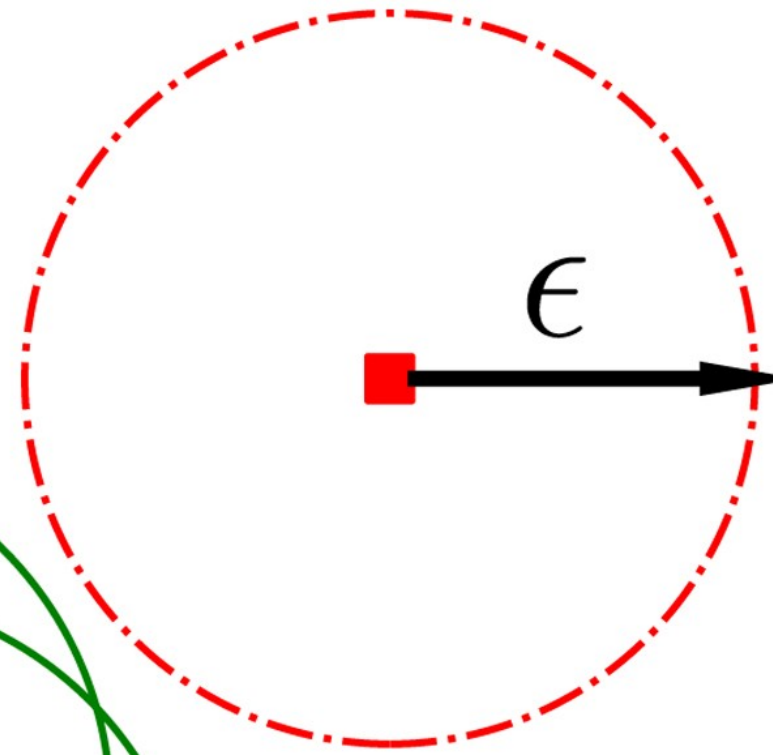# K-means

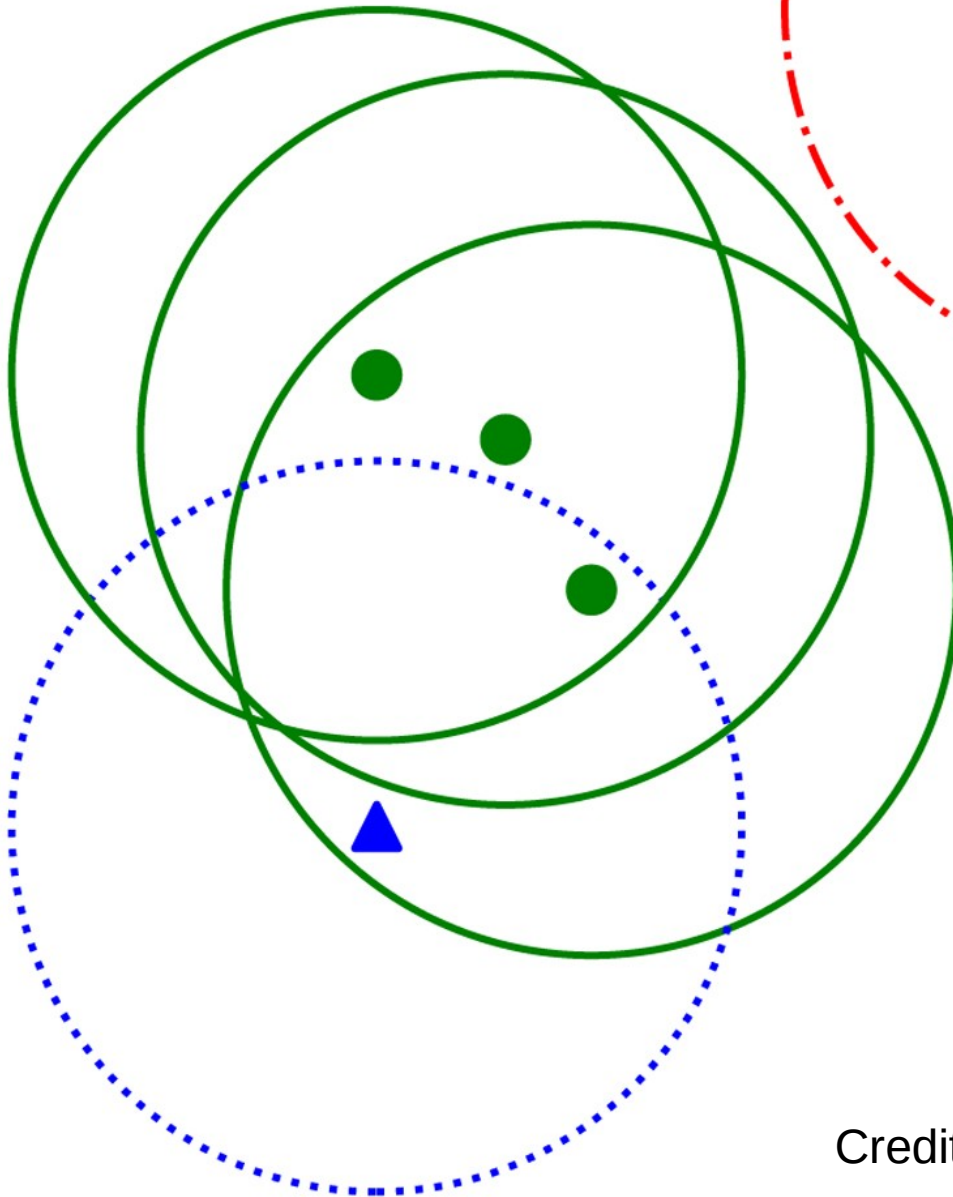
(a) (b) (c)

(d) (e) (f)

Image credit: Michael Jordan

Fig. 4. The top left panel shows the proper motions of stars in the field of NGC 752. The colour-code corresponds to the groups identified by *k*-means clustering in the ($\mu_\alpha*, \mu_\delta, \varpi$) space. The sky distribution of the three highlighted groups is shown in the other panels. Λ is a measurement of spatial clustering, as defined in Eq. [1]. Stars are considered potential cluster members when $\Lambda > 1$.

Cantat-Gaudin+ (2018)

DBSCAN

Two parameters:
Radius of the hypersphere ε
minimum number of sources
(minPts, in this minPts=3)

ϵ